



Contents lists available at ScienceDirect

Gait & Posture

journal homepage: www.elsevier.com/locate/gaitpost



Influence of soft tissue artifacts on the calculated kinematics and kinetics of total knee replacements during sit-to-stand

Mei-Ying Kuo^{a,b,1}, Tsung-Yuan Tsai^{a,1}, Cheng-Chung Lin^a, Tung-Wu Lu^{a,*},
Horng-Chaung Hsu^c, Wu-Chung Shen^d

^aInstitute of Biomedical Engineering, National Taiwan University, Taiwan, ROC

^bDepartment of Physical Therapy, China Medical University, Taiwan, ROC

^cDepartment of Orthopaedic Surgery, China Medical University Hospital, Taiwan, ROC

^dDepartment of Radiology, China Medical University Hospital, Taiwan, ROC

ARTICLE INFO

Article history:

Received 28 April 2010

Received in revised form 1 October 2010

Accepted 9 December 2010

Keywords:

Soft tissue artifact

Fluoroscopy

Skin marker

Motion analysis

Total knee replacement

Kinematics

Kinetics

ABSTRACT

The current study aimed to quantify the soft tissue artifacts of selected markers on the thigh and shank, and their effects on the calculated joint center translations, angles and moments of the knee during sit-to-stand. Ten patients with total knee replacements rose from a chair under simultaneous surveillance of a motion capture system, a force-plate and a fluoroscopy system. The “true” poses of the thigh and shank were defined by those of the femoral and tibial components obtained using a three-dimensional fluoroscopy method. The soft tissue artifacts of the skin markers were calculated as their movement relative to the underlying prosthesis components. The joint center translations, angles and moments at the knee were also calculated separately using skin markers and the registered prosthesis poses. Considerable soft tissue artifacts were found, leading to significantly underestimated flexion and internal rotation angles, and extensor moments, but overestimated joint center translations and adduction. The current study provides accurate data of the kinematics and kinetics of total knee replacements during sit-to-stand. The effects of soft tissue artifacts on the calculated joint center translations, angles and moments were also quantified for the first time in the literature. The results may help in developing guidelines for using skin markers and in establishing databases in the biomechanical assessment of sit-to-stand in patients with total knee replacements.

© 2011 Published by Elsevier B.V.

1. Introduction

Total knee replacement (TKR) has been the main choice of treatment for advanced degenerative osteoarthritis (OA) of the knee over the last few decades. With a good long-term survival rate, improvement of functional recovery has received much attention [1,2]. Therefore, in evaluating TKR designs, it is essential to assess the functional performance of patients during activities of daily living, such as level walking and sit-to-stand (STS). Being a prerequisite to level walking, STS places much greater mechanical demands on the knee joint than level walking, with greater range of motion [3] and moments [4]. Analysis of the STS movement has proven to be a valid tool for assessing the performance of the knee for TKR patients [5], which has been achieved mostly using skin

marker-based three-dimensional (3D) motion analysis techniques [6,7]. A major source of errors in human movement analysis [8] is the associated soft tissue artifacts (STA) which are difficult to eliminate non-invasively [9]. Knowledge of the STA and their effects on the calculated kinematics and kinetics of TKR during STS would be helpful for a better interpretation of the results obtained. It may also help with the development of STA error-compensation methods for reducing their effects.

Previous studies have used invasive approaches to quantify the STA during functional activities [8,10,11], but these methods unacceptably limited the movement itself and restricted the soft tissue displacement relative to the underlying bone. Non-invasive methods based on traditional medical imaging techniques [12,13] are limited to two-dimensional (2D) and/or static measurements. Model-based 3D fluoroscopy methods for measuring *in vivo* 3D kinematics of TKR presented a good opportunity to study the STA non-invasively [14]. Stagni et al. [15] used subjects with TKR to determine the STA of the markers on the lateral aspect of the lower limbs and away from the joints, and their effects on calculated knee angles during functional activities. Unfortunately, the data were limited to those of two subjects, and the effects of the STA on the

* Corresponding author at: Institute of Biomedical Engineering, National Taiwan University, No. 1, Sec. 1, Jen-Ai Road, Taipei 100, Taiwan, ROC.

Tel.: +886 2 33653335; fax: +886 2 33653335.

E-mail address: twlu@ntu.edu.tw (T.-W. Lu).

¹ These authors contributed equally to this work.

calculated moments of the knee were not considered. Moreover, the STA of markers on bony landmarks that are frequently chosen in clinical motion analysis were not included. A recent 3D fluoroscopy method (WEMS) for the registration of a CT-derived bone model and single plane fluoroscopy was proposed for measuring natural knee 3D kinematics [16] and was used to quantify STA in normal subjects during functional activities [17]. However, no study has ever quantified the effects of STA on the calculated kinetics of TKR.

The purposes of this study were to assess *in vivo* the STA of a selection of markers on the thigh and shank that are frequently chosen in clinical motion analysis, to provide accurate data on the joint center positions, angles and moments of the knee, and to evaluate the effects of the STA on these data during STS in patients with TKR by integrating 3D fluoroscopy [16], a force-plate and skin marker-based stereophotogrammetry. It was hypothesized that STA would significantly affect these calculated variables.

2. Materials and methods

2.1. Subjects

Ten subjects (age: 77.7 ± 6.5 years; mass: 63.4 ± 10.1 kg; height: 151.0 ± 7.0 cm), who had received a posterior cruciate ligament-retaining mobile bearing TKR, volunteered to participate in this study. Each subject gave his/her written informed consent before the experiment, which was approved by the Institutional Human Research Ethics Committee. Computer-aided design (CAD) models of the TKR, including femoral, tibial and insert components, were obtained from the manufacturer for subsequent registration with fluoroscopic images. Fifteen infrared retro-reflective markers frequently used in human motion analysis [18] were used to track the motion of the pelvis, and the thigh, shank and foot of the tested limb, Fig. 1. Three additional technical markers were also attached to the thigh (T1, T2, and T3), Fig. 1.

2.2. Functional task

Each subject was asked to sit with the hips abducted at about 30° on an armless, height-adjustable chair and stand up at a self-selected speed while kinematic and kinetic data were measured simultaneously using a 7-camera motion capture system (Vicon, Oxford Metrics, UK), a force-plate (Kistler Instruments, Switzerland) and a fluoroscopy system (Advantx LCA, GE, France), Fig. 1. The height of the chair was set at 115% of the knee-heel distance for each subject. The center of the image intensifier was adjusted to the height of the knee when the subject stood on the force-plate. During STS, the projection beam of the fluoroscopy system was adjusted so that the image plane was slightly oblique with respect to the sagittal plane of the tested knee to avoid overlapping of the bilateral knee joints on the fluoroscopic image, Fig. 1. Data were also collected for each subject during quiet standing.

2.3. Instrumentation

Prior to data collection, the fluoroscopy system was calibrated for image distortions and for the position of the point source X-ray using a purpose-built calibration object [19]. With five retro-reflective markers attached at known positions on the calibration object, the pose of the Vicon coordinate system relative to the fluoroscopy coordinate system was then described by a 3×3 rotation matrix, R_f^v , and a 3×1 translation vector, v_f^v . The residual root-mean-squared error for a marker was 0.7 mm after the spatial registration between the fluoroscopy and the Vicon coordinate systems. During the tests, the fluoroscopic images were obtained at 30 Hz using a PCI bus frame grabber (Foresight, USA), while the Vicon system was operating at 60 Hz. Temporal synchronization of the two systems was achieved using an electrical trigger.

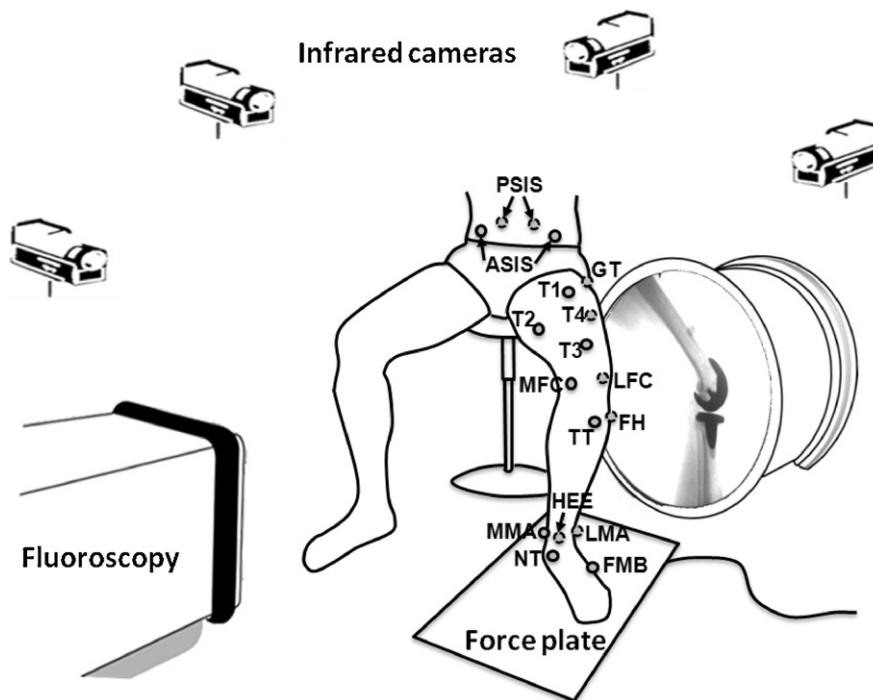


Fig. 1. Schematic diagram showing a subject standing up from a chair while under simultaneous stereophotogrammetry and fluoroscopy system surveillance. Infrared retro-reflective markers were attached on the pelvis and the segments of the tested lower limb (ASIS: anterior superior iliac spine; PSIS: posterior superior iliac spine; GT: greater trochanter; T4: mid-thigh; MFC: medial femoral epicondyle; LFC: lateral femoral epicondyle; FH: head of fibula; TT: tibial tuberosity; MMA: medial malleolus; LMA: lateral malleolus; NT: navicular tuberosity; FMB: fifth metatarsal base; HEE: heel; T1–T3: technical markers).

2.4. Registration

The 3D poses of the TKR components were obtained by registering their CAD models to the corresponding 2D fluoroscopy images using the WEMS method [16]. At each image frame, an optimization procedure was used to find the pose of the component whose projected image best matched the fluoroscopic image according to a similarity measure [16]. A projected image of a TKR component was generated by a perspective projection of the component onto the image plane to form an image resembling a radiograph. The registered component pose was described relative to the fluoroscopy coordinate system in terms of its rotation matrix ($R_f^k(t)$) and translation vector ($v_f^k(t)$). The method was previously evaluated for its accuracy, giving means and standard deviations of errors of -0.08 ± 0.25 mm, 0.01 ± 1.65 mm, and $0.1 \pm 0.33^\circ$ for in-plane translation, out-of-plane translation, and all rotations, respectively [20], similar to those reported in previous studies [14,21]. A graphical user interface was developed to assist with the visualization of the registration process (Fig. 2).

2.5. Data analysis

For inverse dynamics analysis, the pelvis, and the tested thigh, shank and foot were modeled as a 4-link system, each link (segment) embedded with an orthogonal coordinate system with the x-axis, y-axis and z-axis directed anteriorly, superiorly, and to the right, respectively, using relevant skin markers [22]. During subject calibration when no skin movement occurred, TKR coordinate systems were also defined for the thigh and shank based on the registered poses of the femoral and tibial components to coincide with the segment-embedded coordinate systems defined by the skin markers. Meanwhile, the position of a marker relative to the associated TKR coordinate system, denoted as P_k , was taken as the reference for STA estimation during movement. Given the measured marker coordinate relative to the Vicon system ($S_v(t)$), the STA ($E_k(t)$) in terms of the relative movement of the marker along the anterior/posterior (A/P), medial/lateral (M/L) and proximal/distal (P/D) directions in the TKR coordinate system at time t , were calculated as follows.

$$E_k(t) = S_k(t) - P_k \tag{1}$$

$$S_k(t) = R_f^k(t)^T (S_f(t) - v_f^k(t)) \tag{2}$$

$$S_f(t) = R_f^v S_v(t) + v_f^v \tag{3}$$

where $S_k(t)$ and $S_f(t)$ were the current position of the marker relative to the TKR and fluoroscopy coordinate systems, respectively. The markers for STA estimation were the medial and lateral femoral epicondyles (MFC and LFC), thigh markers (T1, T2, T3, and T4), tibial tuberosity (TT), and fibular head (FH) (Fig. 1). The true positions of these markers in the fluoroscopy coordinate system ($P_f(t)$) were obtained as follows.

$$P_f(t) = R_f^k(t)P_k + v_f^k(t) \tag{4}$$

These were then defined as the positions of the so-called virtual bone markers (VBM). The angles of the knee joint were obtained following a z-x-y cardanic rotation sequence, corresponding to flexion/extension (Flex/Ext), adduction/abduction (Add/Abd) and internal/external rotation (IR/ER) [23], using both skin marker and VBM data. The results from the latter were taken as the gold standard. Note that T1, T2 and T3 were not used in the calculation of kinematic and kinetic variables. With the measured ground reaction force (GRF), the knee joint moments about the knee joint center (KJC) were calculated by considering the free bodies of the foot and shank. While the shank was defined separately by skin markers and VBM, the foot was described by skin markers only. Considering the equilibrium of the free body of the foot, its center of gravity (COG) was the only variable that may have been affected by STA of the markers because the ankle joint center was determined by the two malleoli. Being small in size and mass compared to the shank, the foot also had small STA (less than 4.3 mm) [24], which is expected to have small effects on the COG position and thus knee moments. In addition, the foot was not covered by the fluoroscopy. Therefore, the effects of STA of the foot were ignored in the current study. The KJC was defined as the midpoint of the trans-epicondylar axis, and its starting position was obtained in the anatomical position. The displacement of the KJC from the starting position in the shank coordinate system was then defined as the KJC translation. Inertial properties for each body segment were determined using Dempster's coefficients [25]. For inter-subject comparisons, the calculated moments were normalized to body weight (BW) and leg length (LL). All the variables were calculated with respect to the STS cycle defined using the forceplate data [26].

2.6. Statistical analysis

The curves of the STA based on the markers were ensemble-averaged across all subjects, as were the knee angles, translations and moments for both skin markers and VBM data. The means and

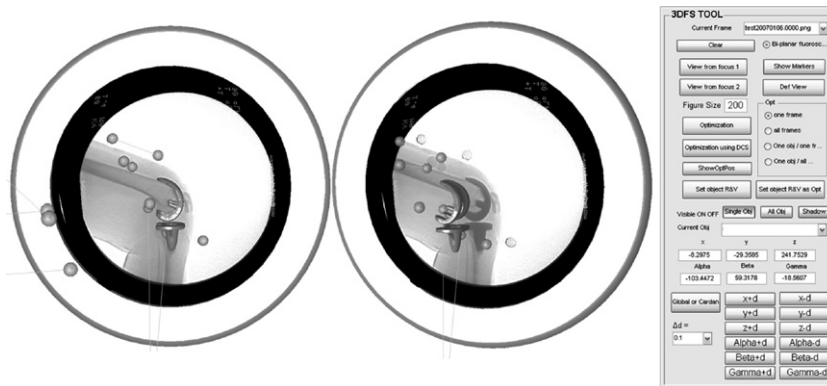


Fig. 2. A graphical user interface (GUI) to assist with the visualization of the registration of the femoral and tibial components of the TKR for their 3D positions and orientations using a 3D fluoroscopy method. The concept of measurement was based on the shape matching of the perspective projection image of the CAD models of the TKR components and the fluoroscopy images. The left image shows the projection of the prosthesis CAD models which were registered to the fluoroscopy image using the WEMS method, while the marker balls shown were obtained from the Vicon system and imported into the program after necessary coordinate transformations. The right image shows the same from an oblique viewpoint.

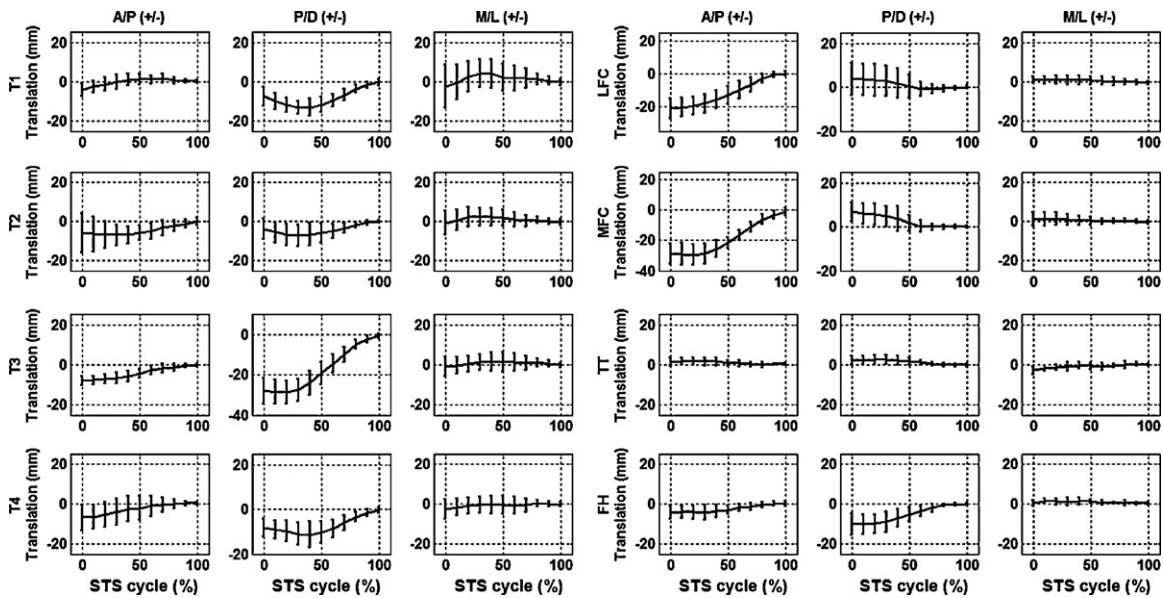


Fig. 3. Mean STA of T1, T2, T3, T4, LFC, MFC, TT and FH across all subjects during sit-to-stand, shown for every 10% of the motion from 0% to 100%. Standard deviations are represented as error bars.

standard deviations at 10% increments during STS were obtained, using GCVSPL [27] for data interpolation when necessary. For comparisons between the results obtained from skin markers and the VBM, a paired *t*-test was used with a significance level of 0.05. SPSS version 10.0 (SPSS Inc., Chicago, USA) was used for all statistical analyses.

3. Results

There were considerable movements of the skin markers relative to the underlying TKR during STS. Different magnitudes and patterns of STA were found for different markers (Fig. 3). As expected, the thigh markers showed greater STA than the shank markers (Fig. 3). The MFC and LFC were displaced posteriorly and

proximally from their true positions when the subjects sat on the chair, and moved anteriorly and distally with the knee extending during STS (Fig. 3). The T1 to T4 markers moved mainly proximally towards the true positions during STS (Fig. 3). On the shank, TT moved within a small range throughout STS (Fig. 3), while FH moved proximally during activity (Fig. 3). None of the markers on the thigh and shank had much translation in the medial/lateral direction.

Significant effects of STA on the knee angles and joint center translations were observed (Fig. 4). During 0–70% of the STS cycle, knee flexion, abduction and internal rotation angles calculated from skin markers were all significantly smaller than the true values (Fig. 4). KJC translations calculated from skin markers were significantly greater than the true values from 0% to 90% of the STS

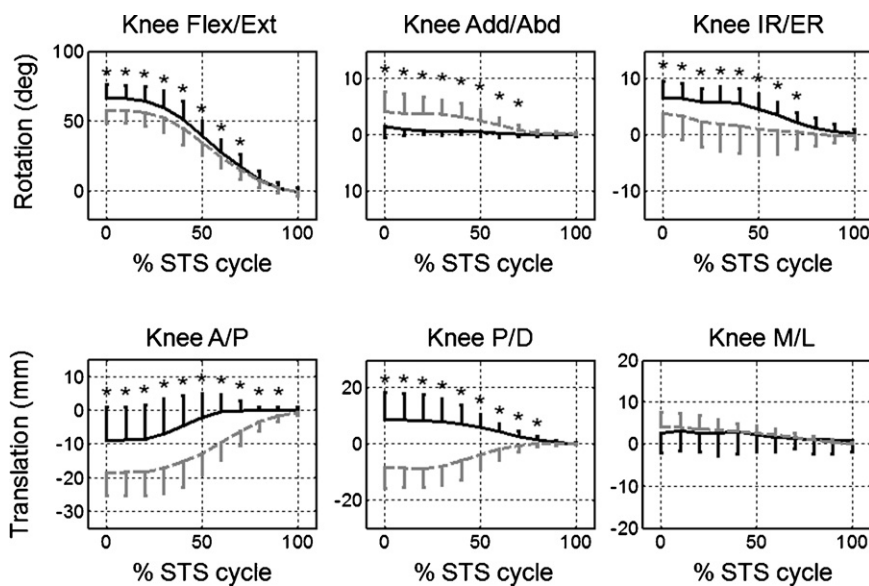


Fig. 4. Means of flexion/extension (Flex/Ext), adduction/abduction (Add/Abd) and internal/external rotation (IR/ER) angles of the knee, measured with skin marker-based motion analysis (gray dashed lines) and the 3D fluoroscopy method (black solid lines). Upper and lower bars represent standard deviations. Means and standard deviations of knee joint translation errors in anterior/posterior (A/P), proximal/distal (P/D) and medial/lateral (M/L) directions with respect to the shank TKR coordinate system are also presented. Stars mark the significant differences of values obtained from the two measurements; the significance level was set to $\alpha = 0.05$.

Table 1

Knee Ext/Flex, Abd/Add and IR/ER moments calculated using skin markers (SM) and VBM from 0% to 100% sit-to-stand at 10% intervals. Differences between the two measurement results are represented by % of the maximum moment calculated by VBM. An asterisk indicates a significant difference ($p < 0.05$).

| %STS | Knee Ext/Flex moment | | | | Knee Abd/Add moment | | | | Knee IR/ER moment | | | |
|------|----------------------|-----------|----------------------------|---------|---------------------|------------|----------------------------|---------|-------------------|------------|----------------------------|---------|
| | SM | TKR | %(SM – TKR)/ (TKR Peak) | p-Value | SM | TKR | %(SM – TKR)/ (TKR Peak) | p-Value | SM | TKR | %(SM – TKR)/ (TKR Peak) | p-Value |
| 0% | 1.4 (1.2) | 1.5 (1.2) | -2.1 (1.8) | 0.008* | 0.3 (0.9) | 0.4 (1.0) | -6.1 (5.8) | 0.037* | 0.0 (0.1) | 0.0 (0.1) | -0.7 (11.7) | 0.739 |
| 10% | 2.0 (1.5) | 2.2 (1.5) | -2.9 (1.6) | 0.002* | 0.2 (0.9) | 0.4 (1.0) | -8.2 (6.7) | 0.026* | 0.0 (0.1) | 0.0 (0.1) | 0.7 (11.4) | 0.570 |
| 20% | 3.7 (2.1) | 4.1 (2.3) | -5.7 (2.3) | 0.002* | 0.0 (0.9) | 0.3 (1.0) | -11.9 (9.5) | 0.030* | 0.0 (0.2) | 0.0 (0.2) | -0.5 (15.2) | 0.698 |
| 30% | 5.0 (2.8) | 5.6 (3.1) | -8.2 (3.7) | 0.003* | -0.1 (1.1) | 0.2 (1.2) | -16.2 (13.9) | 0.028* | 0.0 (0.2) | 0.0 (0.3) | -5.1 (17.8) | 0.914 |
| 40% | 5.8 (2.3) | 6.6 (2.5) | -10.5 (2.6) | 0.000* | -0.3 (1.4) | 0.1 (1.5) | -16.1 (13.6) | 0.010* | 0.0 (0.3) | 0.0 (0.4) | -13.5 (17.5) | 0.319 |
| 50% | 5.1 (2.0) | 5.8 (2.2) | -10.8 (2.5) | 0.000* | -0.3 (1.8) | -0.1 (1.9) | -11.9 (15.2) | 0.044* | 0.0 (0.3) | 0.0 (0.4) | -4.5 (14.8) | 0.963 |
| 60% | 3.8 (2.2) | 4.5 (2.4) | -9.0 (2.2) | 0.001* | -0.3 (2.1) | -0.2 (2.1) | -4.4 (6.9) | 0.095 | -0.1 (0.4) | -0.1 (0.4) | -1.9 (16.2) | 0.717 |
| 70% | 3.0 (2.1) | 3.5 (2.2) | -6.9 (2.6) | 0.001* | -0.3 (2.1) | -0.3 (2.1) | -1.3 (6.3) | 0.702 | -0.1 (0.4) | -0.1 (0.4) | -4.8 (9.4) | 0.688 |
| 80% | 2.0 (1.7) | 2.3 (1.9) | -4.0 (2.8) | 0.008* | -0.2 (2.0) | -0.2 (1.9) | -2.2 (4.7) | 0.455 | 0.0 (0.3) | 0.0 (0.3) | -3.5 (6.1) | 0.295 |
| 90% | 1.5 (1.7) | 1.6 (1.8) | -1.6 (1.8) | 0.037* | 0.0 (2.0) | 0.0 (1.9) | -1.0 (3.8) | 0.989 | 0.0 (0.2) | 0.0 (0.2) | -5.8 (11.5) | 0.213 |
| 100% | 1.0 (1.8) | 1.0 (1.8) | -0.8 (1.0) | 0.102 | 0.2 (2.0) | 0.1 (2.0) | 0.5 (2.0) | 0.201 | 0.0 (0.2) | 0.0 (0.2) | -4.4 (9.8) | 0.372 |

cycle for posterior components and similarly from 0% to 80% for distal components (Fig. 4). No significant differences were found in the M/L component (Fig. 4).

Knee joint moments were significantly underestimated using skin markers, mainly for the extensor and abductor components (Table 1). Knee extensor moments calculated from skin markers were significantly smaller than the true values from 0% to 90% STS cycle, the greatest difference being -10.8% of the true peak moment at 50% STS. Significant differences were also found for abductor moments from 0% to 50% STS, the greatest difference being -16.2% of the true peak moment at 30% STS. Although no significant differences were found for IR/ER moments, differences of -13.5% of the true peak moments were found at 40% STS. In general, STA affected the results of the kinematics and the kinetics of the knee throughout the STS cycle, except during the terminal phase.

4. Discussion

The current study aimed to quantify *in vivo* the STA of a selection of markers on the thigh and shank that are frequently chosen in clinical motion analysis, to provide accurate data on the joint center positions, angles and moments at the knee, and to assess the effects of the STA on these data during STS in patients with TKR. The measured STA of the markers were shown to lead to a significant underestimation of knee joint angles and moments, and an overestimation of joint translations during STS. The marker positions and the definition of the KJC were chosen to follow those frequently adopted in clinical gait analysis [18]. Therefore, the current results are considered to be applicable to most clinical conditions for subjects with TKR.

The studied skin markers showed different STA magnitudes and patterns which resulted in errors in the calculated poses of the body segments and thus the calculated joint kinematics and kinetics. The magnitudes of STA of the thigh markers were greater than those of the shank in the current TKR patients during STS, in agreement with the literature [15]. Similar phenomena were also observed in normal subjects [17]. Therefore, reducing the effects of STA of the thigh is essential for more accurate measurement of the knee motion [10]. In the current study, the under-estimated knee flexion appeared to be a result of a posteriorly tilted shank and an anteriorly tilted thigh determined from the skin markers (Fig. 3), which also led to the over-estimation of the posterior and distal displacement of the KJC. At high knee flexion, according to the z-x-y Cardan angle convention, the abduction/adduction axis was more or less along the longitudinal axis of the thigh and perpendicular to that of the shank. Therefore, the distal displacement of the FH at higher knee flexion led to a laterally tilted shank which further contributed to the over-estimated knee

adduction angle. The STA of the thigh markers, including the greater posterior displacement of MFC than that of the LFC (Fig. 3), resulted in the over-estimated internal rotation of the thigh and thus the observed over-estimation of knee adduction. The over-estimated internal rotation of the thigh also directly explained the under-estimated knee internal rotation angle. Not only were the joint angles affected by the STA, but also the estimated knee joint moments, especially in the sagittal plane. The knee extensor moments were under-estimated by the skin markers which gave a more posteriorly and distally displaced joint center, leading to a reduced lever-arm available to the GRF (Table 1). This is critical as the movement occurred mainly in the sagittal plane, placing greater moments at the knee in this plane than in the other planes (Table 1).

The observed effects of STA on joint center translations, angles and moments at the knee are critical in the study of the kinematics and kinetics of the TKR during STS. The effects of STA were greatest in the peak values of the joint angles and moments (Fig. 4 and Table 1), which were precisely the variables used for statistical analysis in previous studies of TKR during STS using skin marker-based stereophotogrammetry [6,7]. However, these effects have been largely ignored. In the current study, the mean error in the peak knee flexion angle and peak extensor moment were found to be about 10° and 10.5%, respectively, which were close to or even greater than the standard deviations or group differences reported in most of the previous studies [6,7]. While it is not certain whether these errors would affect the statistical results, consideration of STA for more accurate kinematic and kinetic data of the knee will be helpful for reducing Type I errors. Accurate data of the joint angles and moments are also essential in biomechanical applications such as estimating the muscle forces [28] and joint loading [29]. Since it may not be feasible to use 3D fluoroscopy in routine clinical gait analysis for accurate data acquisition, it is desirable to develop STA-compensation techniques, such as the Global Optimization Method [30], in order to reduce the effects of STA on the calculated kinematic and kinetic variables of the knee in future applications. Data obtained from the current study may be helpful for this purpose.

Since the calculated knee moments were directly associated with errors in the joint center translations, comparisons of the performance of different TKR designs with different joint motion patterns may have to consider the potential differences in the effects of STA on the joint center positions. Different joint center definitions may have different effects of STA on the calculated moments. Therefore, a comparative study on the effects of STA on the knee kinetics between various KJC definitions is needed. This will be helpful for the selection of a definition that is less sensitive to STA in TKR subjects during STS. In addition, improper joint types,

such as ball-and-socket assumption for the knee in most motion analysis models, may lead to errors in the calculated joint moments. A more accurate modeling of the knee joint might be helpful for reducing these errors using skin marker-based stereophotogrammetry.

5. Conclusions

The current study provides accurate data of the kinematics and kinetics of TKR during STS using integrated 3D fluoroscopy, a force-plate and stereophotogrammetry. The STA of a selection of skin markers on the thigh and shank that are frequently chosen in clinical motion analysis are reported. Considerable STA were found, leading to significantly underestimated flexion and internal rotation angles, and extensor moments, but overestimated joint center translations and adduction. The results of the study may help in developing guidelines for using skin markers and in establishing databases for the biomechanical assessment of STS in patients with TKR.

Acknowledgments

The authors gratefully acknowledge the financial support from the National Science Council of Taiwan (NSC-94-2213-E-002-112). We also thank the staff of the Medical Imaging Department at China Medical University.

Conflict of interest statement

The authors declare that they have no conflict of interest.

References

- [1] Andriacchi TP, Stanwyck TS, Galante JO. Knee biomechanics and total knee replacement. *J Arthroplasty* 1986;1:211–9.
- [2] Dennis DA, Komistek RD, Mahfouz MR, Haas BD, Stiehl JB. Multicenter determination of in vivo kinematics after total knee arthroplasty. *Clin Orthop Relat Res* 2003;37–57.
- [3] Rowe PJ, Myles CM, Walker C, Nutton R. Knee joint kinematics in gait and other functional activities measured using flexible electrogoniometry: how much knee motion is sufficient for normal daily life? *Gait Posture* 2000;12:143–55.
- [4] Jevsevar D, Riley P, Hodge W, Krebs D. Knee kinematics and kinetics during locomotor activities of daily living in subjects with knee arthroplasty and in healthy control subjects. *Phys Ther* 1993;73:229.
- [5] Boonstra MC, De Waal Malefijt MC, Verdonschot N. How to quantify knee function after total knee arthroplasty? *Knee* 2008;15:390–5.
- [6] Mizner RL, Snyder-Mackler L. Altered loading during walking and sit-to-stand is affected by quadriceps weakness after total knee arthroplasty. *J Orthop Res* 2005;23:1083–90.
- [7] Su FC, Lai KA, Hong WH. Rising from chair after total knee arthroplasty. *Clin Biomech* 1998;13:176–81.
- [8] Cappozzo A, Catani F, Leardini A, Benedetti M, Croce U. Position and orientation in space of bones during movement: experimental artefacts. *Clin Biomech* 1996;11:90–100.
- [9] Leardini A, Chiari A, Della Croce U, Cappozzo A. Human movement analysis using stereophotogrammetry. Part 3. Soft tissue artifact assessment and compensation. *Gait Posture* 2005;21:212–25.
- [10] Reinschmidt C, van den Bogert AJ, Nigg BM, Lundberg A, Murphy N. Effect of skin movement on the analysis of skeletal knee joint motion during running. *J Biomech* 1997;30:729–32.
- [11] Manal K, McClay I, Stanhope S, Richards J, Galinat B. Comparison of surface mounted markers and attachment methods in estimating tibial rotations during walking: an in vivo study. *Gait Posture* 2000;11:38–45.
- [12] Sangeux M, Marin F, Charleux F, Durselen L, Ho Ba Tho MC. Quantification of the 3D relative movement of external marker sets vs. bones based on magnetic resonance imaging. *Clin Biomech* 2006;21:984–91.
- [13] Sati M, de Guise JA, Larouche S, Drouin G. Quantitative assessment of skin-bone movement at the knee. *Knee* 1996;3:121–38.
- [14] Banks SA, Hodge WA. Accurate measurement of three-dimensional knee replacement kinematics using single-plane fluoroscopy. *IEEE Trans Biomed Eng* 1996;43:638–49.
- [15] Stagni R, Fantozzi S, Cappello A, Leardini A. Quantification of soft tissue artefact in motion analysis by combining 3D fluoroscopy and stereophotogrammetry: a study on two subjects. *Clin Biomech* 2005;20:320–9.
- [16] Tsai TY, Lu TW, Chen CM, Kuo MY, Hsu HC. A volumetric model-based 2D to 3D registration method for measuring kinematics of natural knees with single-plane fluoroscopy. *Med Phys* 2010;37:1273–84.
- [17] Tsai TY, Lu TW, Kuo MY, Hsu HC. Quantification of three-dimensional movement of skin markers relative to the underlying bones during functional activities. *Biomed Eng Appl Basis Commun* 2009;21:223–32.
- [18] Cappozzo A, Catani F, Della Croce U, Leardini A. Position and orientation in space of bones during movement: anatomical frame definition and determination. *Clin Biomech* 1995;10:171–8.
- [19] Lu TW, Tsai TY, Kuo MY, Hsu HC, Chen HL. In vivo three-dimensional kinematics of the normal knee during active extension under unloaded and loaded conditions using single-plane fluoroscopy. *Med Eng Phys* 2008;30:1004–12.
- [20] Tsai, TY. Development of a 3D fluoroscopy method and its integration with stereophotogrammetry to study the effects of soft tissue artifacts on the calculated mechanical variables of the knee during functional activities. Ph.D. Thesis. Taipei, Taiwan: National Taiwan University; 2010.
- [21] Yamazaki T, Watanabe T, Nakajima Y, Sugamoto K, Tomita T, Yoshikawa H, et al. Improvement of depth position in 2-D/3-D registration of knee implants using single-plane fluoroscopy. *IEEE Trans Med Imaging* 2004;23:602–12.
- [22] Lu TW. Geometric and mechanical modelling of the human locomotor system. D.Phil. Thesis. Oxford, UK: University of Oxford; 1997.
- [23] Cole GK, Nigg BM, Ronsky JL, Yeadon MR. Application of the joint coordinate system to three-dimensional joint attitude and movement representation: a standardization proposal. *J Biomech* 1993;115:344–9.
- [24] Tranberg R, Karlsson D. The relative skin movement of the foot: a 2-D roentgen photogrammetry study. *Clin Biomech* 1998;13:71–6.
- [25] Winter DA. *Biomechanics and motor control of human movement*. New York: John Wiley & Sons; 2009.
- [26] Hesse S, Schauer M, Jahnke MT. Standing-up in healthy subjects: symmetry of weight distribution and lateral displacement of the centre of mass as related to limb dominance. *Gait Posture* 1996;4:287–92.
- [27] Woltring HJ. A Fortran package for generalized, cross-validatory spline smoothing and differentiation. *Adv Eng Softw* 1986;8:104–13.
- [28] Tsirakos D, Baltzopoulos V, Bartlett R. Inverse optimization: functional and physiological considerations related to the force-sharing problem. *Crit Rev Biomed Eng* 1997;25:371–407.
- [29] Lu TW, O'Connor JJ, Taylor SJ, Walker PS. Validation of a lower limb model with in vivo femoral forces telemetered from two subjects. *J Biomech* 1998;31:63–9.
- [30] Lu TW, O'Connor JJ. Bone position estimation from skin marker co-ordinates using global optimisation with joint constraints. *J Biomech* 1999;32:129–34.